NIH Public Access
Author Manuscript
Biomaterials. Author manuscript; available in PMC 2013 March 03.

Published in final edited form as:
Biomaterials. 2012 June ; 33(18): 4752–4761. doi:10.1016/j.biomaterials.2012.03.023.

Therapeutic effect of orally administered microencapsulated oxaliplatin for colorectal cancer

Aleksandra M. Urbanska[a,c], **Emmanouil D. Karagiannis**[a,c], **Gonzalo Guajardo**[a], **Robert S. Langer**[a,b,c,d], and **Daniel G. Anderson**[a,b,c,d,*]

[a]The David H. Koch Institute for Integrative Cancer Research, Massachusetts Institute of Technology, Cambridge, MA 02142, USA

[b]Department of Anesthesiology, Children's Hospital Boston, Boston, MA 02115, USA

[c]Department of Chemical Engineering, Massachusetts Institute of Technology, 77 Massachusetts Avenue, Cambridge, MA 02139, USA

[d]Harvard-MIT Division of Health Science Technology, Massachusetts Institute of Technology, 45 Carleton Street, Building E25-342, Cambridge, MA 02142, USA

Abstract

Colorectal cancer is a significant source of morbidity and mortality in the United States and other Western countries. Oral delivery of therapeutics remains the most patient accepted form of medication. The development of an oral delivery formulation for local delivery of chemotherapeutics in the gastrointestinal tract can potentially alleviate the adverse side effects including systemic cytotoxicity, as well as focus therapy to the lesions. Here we develop an oral formulation of the chemotherapeutic drug oxaliplatin for the treatment of colorectal cancer. Oxaliplatin was encapsulated in pH sensitive, mucoadhesive chitosan-coated alginate microspheres. The microparticles were formulated to release the chemotherapeutics after passing through the acidic gastric environment thus targeting the intestinal tract. *In vivo*, these particles substantially reduced the tumor burden in an orthotopic mouse model of colorectal cancer, and reduced mortality.

Keywords

Oxaliplatin; Intestinal tumorigenesis; Colon cancer; Oral delivery; Alginate

1. Introduction

Despite considerable efforts to improve early diagnosis and treatment, colorectal cancer remains the third most common cancer in the world [1]. Platinum-based compounds such as *cis*-diamminedichloroplatinum(II) (CDDP), carboplatin (CBDCA) and oxaliplatin (LOHP) are important anticancer drugs [2]. Unfortunately, their therapeutic utility is limited by drug resistance in tumors [3] and systemic toxicity [4,5]. In colorectal cancer therapy, as it is in other cancers, biodistribution to tumor tissue can be limited and not reach effective concentrations [6,7].

© 2012 Published by Elsevier Ltd.

*Corresponding author. The David H. Koch Institute for Integrative Cancer Research, Massachusetts Institute of Technology, Cambridge, MA 02142, USA. dgander@mit.edu (D.G. Anderson).

NIH-PA Author Manuscript
NIH-PA Author Manuscript
NIH-PA Author Manuscript

NIH-PA Author Manuscript

NIH-PA Author Manuscript

NIH-PA Author Manuscript

Oral administration of drugs is the one of the most convenient and patient accepted methods of drug delivery. However, the gastrointestinal microenvironment presents many delivery challenges including the acidic conditions of the stomach, the proteolytic activity of the gastrointestinal tract due to the presence of digestive enzymes, and the high density of bacterial species. While intravenous (i.v.) administration of chemotherapeutics is common practice, the oral route provides an anatomical advantage for delivering such agents, as it permits direct access to the luminal tissue affected by many diseases.

One promising method for oral drug delivery involves the use of mucoadhesive biomaterials such as chitosan and alginate. Chitosan's mucoadhesion has been used in various clinical applications including nasal administration of drugs [8], wound healing [9], as well as transmucosal insulin delivery [10]. Similarly, alginates have been used as substrates for vaginal delivery of siRNA [11], in particulate formulations for controlled gastric drug release [12] or as patches for post-surgical tissue adhesion barriers [13].

Alginates are composed of α-L-guluronic acid (GG) and β-D-mannuronic acid (MM)residues at varying proportions of GG-, MM-, and GM-blocks [14]. They are drug excipients, and have been used as a matrix for cells in the field of tissue engineering. Alginic acid and its salts are considered to be Generally Recognized as Safe (GRAS) according to the Food Additive Status List [15] and have been used in the food industry as thickening agent, preservative, antioxidant, flavoring agents, as well as an encapsulant material [16]. The biological activity of drugs encapsulated in particles formulated with such materials can be retained through the calcium-cross-linked alginate encapsulation process [17] and alginate is non-toxic and biodegradable when given orally [18,19]. Moreover, alginates can be prepared in a neutral or charged form, making them compatible with a variety of other materials, and altering their material properties [20–22]. Chitosan is another polymer which demonstrated utility in humans, and is biodegradable, mucoadhesive and relatively non-toxic in certain applications [23].

Here we report an oral formulation for delivery of oxaliplatin to colorectal cancer tissue. Such a formulation can be a significant alternative to the standard chemotherapeutic drug delivery strategies. It can reduce the systemic level cytotoxicity; it can provide a patient friendly method of drug administration as well as provide direct access to the GI tract tissues of interest.

Thus the formulation developed here may have potential therapeutic applications for a variety of diseases including colorectal cancer, as well as other GI related disorders such as Irritable Bowel Syndrome (IBS), Crohn's disease, and Colitis.

2. Methods

2.1. Preparation of the formulations

2.1.1. Formulation containing oxaliplatin—Oxaliplatin (Biotang Inc., Waltham, MA) was dissolved in PBS using sonication, formulated with lipidoid nanoparticles and blended with sterile 2% alginate solution. The mixture was loaded into a syringe and mounted onto a pump. The entire procedure was performed under sterile conditions. Alginate microcapsules were prepared aseptically using Harvard Apparatus PicoPlus Elite pump attached to a voltage source. Microcapsules were collected into 0.1 M $CaCl_2$ bath and left for 30 min before washing twice with PBS. A solution of 0.5% chitosan was prepared by dissolving it in 0.1% solution of acetic acid and at pH 5.2. The final dissolved mixture was sterile filtered with 0.22 um. Parameters for microencapsulation were as follows: hardening time in CaCl2 – 30 min, coating time with 0.5% chitosan – 30 min, needle gauge – 18g, rate – 200 ul/min, voltage - 10 kV and current 2 amp. Microencapsulation yielded homogenous spheres of 80 ±

NIH-PA Author Manuscript

NIH-PA Author Manuscript

NIH-PA Author Manuscript

28 mm in diameter. Prepared microparticles were washed with sterile PBS and stored at 4 °C until used.

2.1.2. Formulation containing lipidoid nanoparticles—The C12-200 lipidoid nanoparticles were formulated from lipidoid, cholesterol, and a polyethylene glycol modified lipid as previously described [25]. Stock solutions of lipidoid, cholesterol (Sigma-Aldrich), and a PEG lipid (N-palmitoyl-sphingosine-1-[succinyl[methoxy(polyethylene glycol)2000]], MW 2634, Avanti Polar Lipids) were prepared in absolute ethanol at concentrations of 100, 15, and 100 mg/mL, respectively. The components were then combined and vortexed to yield weight fractions of 52:20:28. The ethanol mixture was then added drop wise to 200 mM sodium acetate buffer (pH 5) in a glass vial with concurrent stirring to spontaneously form empty lipidoid nanoparticles. After the particle formulation they were incubated at room temperature for 30 min. The formulations were then dialyzed against PBS in a 10 kDaMWCO dialysis cassette (Pierce, Rockford, IL) for 2 h. Following buffer exchange, oxaliplatin solution in PBS at a concentration of 55 mg/kg was added to a sample, each formulation was used for particle characterization; the drug entrapment was estimated using UV spectroscopy and the mean particle size was quantified by dynamic light scattering (ZetaPALS, Brookhaven Instruments).

2.2. Animals

All procedures used in animal studies were approved by the Institutional Animal Care and Use Committee and were consistent with local, state and federal regulations as applicable.

Male C57BL/6J-*Apc*$^{Min/+}$ mice, weighing w23 g, were purchased from the Jackson Laboratory (Bar Harbor, ME, USA). The animals were kept in the Koch Institute Animal Facility on a 12 h light–dark cycle and controlled humidity and temperature. They were allowed sterile water and the laboratory rodent diet from Harlan *ad libitum*. Animals overall health was monitored daily. The protocol was approved by the Animal Care Committee of MIT and animals were cared for in accord with the Comparative Animal Care (CAC) guidelines.

2.3. Animal protocol

Male C57BL/6J-*Apc*$^{Min/+}$ mice were used. They were separated into two experimental groups: Control - animals gavaged with empty alginate-chitosan (AC) microcapsules suspended in PBS, Treatment group – animals gavaged with AC microencapsulated lipidoid and oxaliplatin nanoparticles suspended in PBS. Upon arrival, animals were randomly block assigned and allowed one week of acclimatization period. There were 10 animals per group. Animals were weighed individually every week; the bleed from saphenous veinwas performed every 3 weeks and fecal samples were collected weekly throughout the experiment. If any animal during experiment had a body weight decrease of over 20% within a week they were scheduled for euthanasia. Mice were CO_2 euthanized at the end of the experiment. Cardiac blood was collected and the entire small intestine, cecum and colon were removed. Spleens were removed, weighted and measured. The rest of the organ was made into a ‘Swiss-roll’, placed in a separate histology cassette and preserved in 4% neutral buffered formalin solution.

2.4. Intestinal histopathology

After excising small intestine, cecum and colon, tissues were fixed with formaldehyde. A formaldehyde solution (final concentration, 10% [*wt/vol*] paraformaldehyde) in phosphate-buffered saline (130 mM sodium chloride, 10 mM sodium phosphate buffer, pH 7.2) was used. The material was then incubated overnight in the refrigerator (4 °C) for fixation. After fixation tissues were transferred to 70% ethanol. Sections with a thickness of 6 mmwere cut

NIH-PA Author Manuscript

NIH-PA Author Manuscript

NIH-PA Author Manuscript

in the cryostat with a manual cryotome. Sections were directly picked up onto an adhesive, electrostatically charged microscope slides (Fisherbrand Superfrost Plus Microscope Slides, USA). This was done immediately after the microscope slides were introduced into the cryostat. It was important that the microscope slides be at room temperature during this procedure in order to allow adhesion and smoothing out of the thawing microtomic sections. Subsequently, the mounted tissue holder was incubated at −22 °C for 1 h (precooling) in the cryostat. Adenomas were visualized by staining tissue with hematoxylin and eosin stains. They were identified, counted and measured with the aid of transmitted light microscope Evos xl AMG, with imaging software. To assess mucin production, slides were treated with Alcian Blue (pH2.5) for 5 min, then mounted using standard techniques. Slides were then stored at −80 °C prior to immunostaining.

2.5. Immunohistochemistry

For immunohistochemistry staining sections were deparafinized in a series of xylene and ethanol solutions (100%, 90%, 80% and 70%) followed by a hydration with distilled water.

Immunostaining was performed by the avidin-biotin complex technique using the Millipore IHC SelectRTM HRP/DAB kit. Briefly, tissues were pretreated using a citrate buffer, pH 6.0 and blocked with normal serum from the kit for 10 min 3% hydrogen peroxidase treatment was applied to samples for 2 min. Samples were rinsed with PBS buffer and incubated with 2% normal serum in PBS to avoid background staining. The slices were incubated with the biotinylated secondary antibody for 10 min, rinsed and applied with Streptavidin-HRP solution for 10 min. Negative control samples were produced by incubating the samples in TBS plus 1% BSA without either of the biotinylated primary antibodies.

Nitrotyrosine antibody (Cayman, Ann Arbor, ME) was used at a dilution of 1:200. To access mucin production, slides were treated with Alcian Blue pH 2.5 for 5 min, and then mounted using standard techniques.

Terminal deoxynucleotidyl transferase-mediated dUTP nick end labeling (TUNEL) assay was done with an *in situ* cell death detection kit (Roche, Branchburg, NJ). Briefly, deparafinization of tissues was performed as described before. The slides were hydrated in PBS buffer for 30 min. Subsequently, tissues were digested for 30 min with Proteinase K (Roche, Branchburg, NJ). Slides were rinsed with PBS twice. Label solution was added to enzyme solution and mixed to equilibrate components. Reaction mixture was added onto each slide and the sections were incubated for 60 min in a humidified atmosphere chamber in the dark. Lack of TdT in the TUNEL mix completely abolished labeling under all working conditions and therefore served as TUNEL negative control. Tissue sections were analyzed in a drop of PBS buffer under a fluorescence microscopy at an excitation wavelength of 450 nm and detection range of 515–565 nm. Further, signal conversion was performed using converter-POD; slides were incubated for 30 min at RT in a humidified atmosphere chamber in the dark at RT. Slides were rinsed 3 times with PBS and 0.05% 3-3′-diaminobenzidine tetrahydrochloride (DAB) substrate was added onto each slide and incubated for 10 min at RT. Next, slides were washed with PBS buffer 3 times and counterstained with hemotoxylin and eosin for w60 s each. The samples were mounted in an aqueous solution (VectaMount AQ, Vector Laboratories, Inc.) and covered with a coverslip to analyze under fluorescent microscope Evos fl AMG, with imaging software.

All of the kits were used according to the manufacturers' instructions.

2.6. Polyp counting

Polyp scoringwas performed by a person blinded to the experimental setup. The adenomas observed were divided into two categories based on the size: gastrointestinal intraepithelial

NIH-PA Author Manuscript

NIH-PA Author Manuscript

NIH-PA Author Manuscript

neoplasia (GIN)(<1 mm) and adenoma (>1 mm). In addition, the counted polyps were graded as follows: (small intestines) no polyps: score 0; up to 5: score 1; up to 10: score 2; from 11 to 15: score 3 and above 15: score 4; (large intestines) no polyps: score 0; up to 1: score 1; up to 2: score 2; up to 3 score: 3; up to 4 score: 4 and above 5: score 5.

The standards for the histological assessment were established from the MMHCC-sponsored symposium.

2.7. Fecal extraction; lactoferrin and C-reactive protein determination

Feces were collected weekly throughout the experiment and the analysis was averaged per group per cage. Fecal extractionwas performed as previously described [26] with the following modifications. 800 μL of sample were added to 400 μL of 3 M NaOH and heated at 95 °C for 2hr. A mouse Lactoferrin Elisa (TSZ Elisa, Framingham, MA) was used to determine the concentration of the protein and C-Reactive Protein concentration was determined using a mouse Elisa kit from Life Diagnostics, Inc (West Chester, PA).

2.8. Statistical analysis

Data were analyzed using a one-way analysis of variance with Student Newman-Keuls post hoc analysis. All data were analyzed using a commercial software SigmaStat; SPSS. Data were expressed as means ± standard error of the mean. Data were considered significant at $p < 0.05$.

3. Results

3.1. Survival, body weight and rectal bleeding

One characteristic of colorectal tumor progression is patient weight reduction and the presence of blood in the stool [27,28]. Body weight decrease is attributed to chronic constipation and abdominal pain whereas bleeding can be caused by the friction and shear of the stool with the projecting interstitial tumors [29,30]. Given the significance of these features to the disease progression, we monitored, on weekly basis, the animal body weight and rectal bleeding.

In Fig. 1A we plot the progression of the body weight for the 17 weeks of treatment for two animal groups, control group receiving empty AC microcapsules and treatment group receiving microencapsulated lipidoid nanoparitcles containing oxaliplatin. All animals gained weight steadily up to the 6th week. For the next two weeks, animals from the control group lost weight however, with final body weight observed, 22.58 ± 1.2 g. Animals from treatment group continued to gain weight and had terminal weights of 26.42 ± 1.6 g. During daily health monitoring, we examined animal integument, erythema, haircoat condition, status of hydration and pruritus. There were no severe cases observed apart from few animals being dehydrated, all of which would receive subqutaneously injection of sterile PBS. Based on daily observations of animal overall health, we noticed lack of coordination along with slight body shivering and hunched in some animals of control group receiving empty AC microcapsules suspended in saline. These animals also had a higher incidence of rectal bleeding/blood in the stool when compared to the treatment group. They were characterized by lack of energy and decreased motion rate. They acted restless with curled bodies and lowered heads. No changes in muscular disturbances such as generalized tremors, lip drooping and/or paralysis were noted in any animal.

3.2. Inflammation biomarkers and intestinal tumorigenesis

Many cancers are associated with chronic inflammation [31]. There are many chemokines and cytokines involved in the recruitment and trafficking of inflammatory cells to the sites

NIH-PA Author Manuscript

NIH-PA Author Manuscript

NIH-PA Author Manuscript

of tumor development [32]. The expression of various chemokines by intestinal cells, particularly those of the epithelium, is a key to the development of an inflammatory response. In such situation the macrophages detect tumor antigens and secrete IL-12, which activates T cells and leads to the secretion of IFN-γ and TNF-α [33,34]. Those chemokines in turn stimulate the tissue residing or recruited macrophages to produce proinflammatory cytokines like IL-1β, TNF-α and IL-6. Such cytokines can in turn trigger the upregulation of secondary inflammation markers like lactoferrin and C-reactive protein. Here we quantify the expression of these inflammation markers and follow their levels along the progression of the disease.

During the 17-week experimental period, collected blood serum was used to measure the levels of inflammatory interleukin-6 and -12. The concentration levels were significantly higher in control group compared to treatment group (Fig. 2A,B). For IL-12, at the time of sacrifice the average levels were 47.55 ± 10.06 pg/mL for control and 20.71 ± 4.65 pg/mL, and for treatment group. In addition, the levels of proinflammatory cytokine, IL-6 were measured in serum. They were 28.23 ± 3.84 pg/mL for control and 17.21 ± 1.17 pg/mL for treated animals at the time of sacrifice.

Lactoferrin was measured as a marker for fecal leukocytes. This test is more sensitive than microscopy for identifying leukocytes and discriminates between inflammatory and non-inflammatory bowel processes [35]. Lactoferrin concentration was determined from fecal samples. The averages levels at the time of sacrifice were 33.11 ± 2.28 pg/mL for control and 23.15 ± 1.29 pg/mL for treatment animals at the time of sacrifice, and; Fig. 3A.

Another marker for acute phase inflammation is C-reactive protein (CRP). CRP is synthesized in the liver in response to cytokines like IL-6 and its increased levels can be indicative of the inflammatory state [36,37]. C-reactive protein levels in the fecal samples were determined by enzyme-linked immunosorbent assay, no significant changes were observed within groups: 77.69 ± 4.13 ng/mL in control group, compared to 58.90 ± 6.28 ng/mL in oxaliplatin group at the 17th week of treatment; Fig. 3B.

3.3. Morphological characteristics of tumors

We performed histopathology analysis, using H&E staining, of the different GI compartments namely the small intestine, cecum and colon, of treated animals. Tumors were scored and classified according to their size. As shown in Fig. 4, the tumors found in control group animals were predominantly tubular adenomas with a pedunculated morphology greatly protruding into the colonic lumen. However, there was no evidence of invasion of the underlying submucosa by neoplastic epithelial cells, and therefore none of the adenomas examined were classified as being carcinomas. Within control group there were high-grade dysplasia adenomas with foci of intraluminal necrosis. A representative tumor of the small intestine shows pedunculated (polypoid) adenoma with a high-grade of dysplasia (Fig. 4 – top panel, indicated by arrows). A representative animal from oxaliplatin treatment group depicts gastrointestinal intraepithelial neoplasia (microadenomas) of small intestine (Fig. 4-bottom panel).

Furthermore we observed an increase in nuclear/cytoplasmic ratio and the nuclear crowding at the lamina propria/crypt within oxaliplatin group in the small, colon and cecum. In both groups, tumors in the small intestine were mostly less than 1 mm in diameter. The control group animals had significantly higher polyp count, on average 15.2 in the small intestine, 0.33 in cecum and 1 in colon. In the oxaliplatin treatment group we counted 10.1 tumors in the small intestine, 0.11 in cecum and 0.44 in colon; Table 1A. The number of tumors was also scored according to a 0e5 scale (Materials and Methods), with 0 the no tumor condition and 5 the most advanced disease state. The scores are presented in Table 1B. Finally,

NIH-PA Author Manuscript

NIH-PA Author Manuscript

NIH-PA Author Manuscript

spleens' weights and lengths were recorded, Table 1C. They were on average in control group 2.33 ± 0.25 cm in length and 485 ± 8.21 mg in weight. In the oxaliplatin group they were 2.28 ± 0.14 cm and 404 ± 10.08 mg.

3.4. Immunohistochemistry

Using terminal deoxynucleotidyl transferase-mediated dUTP nick end labeling (TUNEL), an *in situ* method for detecting the 3′-OH ends of DNA exposed during the internucleosomal cleavage that occurs during apoptosis we evaluated the apoptotic state of tumor cells in the small and large intestinal tissues. We expect an increased number of apoptotic cells in the conditions that we deliver oxaliplatin. In the tumor of the untreated mice we found only few fluorescently labeled cells, primarily located on the peripheral surface of the tumors, where the oldest cells reside, Fig. 5A. When compared to the oxaliplatin treatment condition we observed fluorescently labeled cells throughout the tumor, Fig. 5B.

Also, we investigated the mucin production by staining with alcian blue to detect mucous-producing Goblet cells. Decreased mucin levels are correlated with a pathologic condition. The greatest amounts of mucin producing cells were found in the normal intestinal tissues, Fig. 5D whereas significantly reduced numbers were detected in the areas with tumors, Fig. 5C.

Nitrotyrosine levels in the small intestine of control and treatment group were evaluated in a representative animal. Nitrotyrosine is a product of tyrosine nitration mediated by reactive nitrogen species such as peroxynitrite anion and nitrogen dioxide. It is detected in large number of pathological conditions and is considered a marker of nitric oxide dependent nitrative stress. There was an increased level of nitrotyrosine in the microvilli of the small intestine of untreated animal, Fig. 5E relative to the small intestine stained with cells expressing nitric oxide only at the peaks of microvilli, Fig. 5F.

To further investigate the inflammatory changes, we analyzed intestinal tissues to see whether there was an increase in the cycling/proliferating cells within the small and large intestine, and to determine the potential treatment effect on recruitment of T cells as well as cell proliferation and apoptosis, Fig. 6A (small intestine) and B (colon).We assessed the inflammatory changes in the tumors of the control and oxaliplatin treatment animals found in the intestine and colons by immunohistochemistry using of cyclooxygenase-2 (Cox-2), cleaved caspase-3, Ki-67 and mdm-2 antibodies. Overall there was a greater concentration of Cox-2 expressing cells in the control group versus treatment. Cleaved caspase-3 expressing cells, apoptotic cells, were mostly located in the tumors of oxaliplatin treatment animals. The Ki-67 staining has not revealed significant differences between cell populations between groups. Mdm-2 expressing cells were fewer, scarcely located within tumors of treatment group animals.

4. Discussion

Platinum containing chemotherapeutics are a standard therapy for many patients [38–40]. However, to our knowledge, the utility of these drugs for colorectal cancer therapy following oral administration has not been demonstrated. Here we developed an oral formulation of oxaliplatin for colorectal cancer therapy. Our findings demonstrate that in mice, oral formulations of oxaliplatin can be developed with potential utility against colorectal cancer.

This study used an established mouse model of intestinal tumorigenesis with the multiple intestinal neoplasia (Min) mutation, a heterozygous nonsense mutation at codon 850 of the *Apc* gene [24,41]. After somatic mutation of the second *Apc* allele, Min mice develop

NIH-PA Author Manuscript

NIH-PA Author Manuscript

NIH-PA Author Manuscript

multiple polyps or adenomas in the small intestine as well as a small number of colonic adenomas at around 2–3 months of age [41]. This animal model is the most widely used genetically engineered mouse model for cancer studies that involve the gastrointestinal tract [42,43]. Among the organs examined in this study, there was only one malignant tumor (adenocarcinoma) found in the small intestine of a control animal. The nuclei were enlarged and pleomorphic with variable loss of their polarity. The glandular structure was distorted and resembled that seen in overt colonic carcinoma. The highest tissue damage was observed in the colon of control group animals under the same conditions as applied to the other tissues. We hypothesize that this reflects the fact that the colonic wall, including the mucosa and the submucosa, is much thinner than that of the other organs.

Most of the adenomas found were sessile and broad-based and were composed of papillary projections of lamina propria covered by an epithelium. There were significantly less adenomas found in the ceca. The greatest loss in mucin secretion was displayed in severely dysplastic glands of control group animals sacrificed at the 17th week of the experiment. The glands were closely packed and a structural atypia, e.g. "back to back" arrangement was more prominent. Nuclei were plump but still uniform and smaller than those in carcinomatous glands. Cytological abnormalities detected included cellular and nuclear pleiomorphism and loss of polarity. Architectural abnormalities included the presence of intraglandular papillary projections and of cribriform and solid epithelial areas. There were, however, no major differences in animal tissues collected from animals sacrificed at different time periods due to premature excess loss of body weight. The tumors found in the treatment group showed some features of papillary carcinoma-grooved nuclei and papillary architecture, but these were not consistent. Future work could incorporate additional cellular markers to reveal immunocytochemical indices of tumor growth dynamics such as proliferation-associated antigens (e.g. CCL2, PCNA) and to examine reciprocal correlations between the intensity of apoptosis and the expression of such pro- and anti-apoptotic cell markers as caspase-3 (cas-3) and Ki-67 antigen.

Many cancers are associated with a chronic inflammatory process [44–46]. Inflammatory bowel disease, including both ulcerative colitis and Crohn’s disease, has a well-established association with the development of colorectal cancer [47]. In contrast to colorectal cancers with a well-defined genetic basis like familial adenomatous polyposis, it appears that chronic inflammation predisposes to the development of colorectal cancers in the setting of inflammatory bowel disease [48]. This is supported by the fact that for example anti-inflammatory agents decrease the risk of developing colorectal cancer in inflammatory GI diseases. The chronic inflammatory response represents a fine balance between active inflammation, repair, and degradation that occurs in response to a persistent biochemical stimulus over a prolonged period of time. Activation of leukocytes in response to such an ongoing stimulus leads to the production of chemokines, cytokines, and reactive oxygen species, resulting in accumulated tissue destruction and subsequent attempts at healing via remodeling, angiogenesis, and connective tissue replacement [48]. Our results confirm the previously reported studies which found increased IL-6 immunoreactivity in cancerous lesions when compared to normal colon mucosa and that IL-6 concentrations correlated with tumor tissue concentrations and proliferative activity [31,34,49]. The differences in inflammation levels among the treatment groups could be the result of stimulation of mucosal barrier function, decreased binding to or penetration of pathogens to mucosal surfaces, or altering immunoregulation (decreasing proinflammatory and promoting protective molecules). Another marker for reduced inflammation levels in the treatment group is IL-12. IL-12 is a chemokine expressed by various leukocytes and lymphocytes like dendritic cells, macrophages and B cells in response to stimulation by various antigens.

NIH-PA Author Manuscript

NIH-PA Author Manuscript

NIH-PA Author Manuscript

Lactoferrin, a multifunctional protein that is part of the innate defense against infection and inflammation is present in milk, saliva and other exocrine secretions as well as in neutrophil granules. It has a number of biological functions, including antimicrobial and immunomodulatory effects in vitro and in vivo [50]. Its levels are elevated in fecal samples in inflammatory bowel disease patients [51,52]. During intestinal inflammation, leukocytes infiltrate the mucosa, which results in increased lactoferrin in the feces [52,53]. We observed a decrease in concentration levels throughout the experiment in the treatment group, with significant difference in the last week (Fig. 3a). In addition, we quantified the levels of C-reactive protein, a well-known acute-phase marker of inflammation in the body and it has been reported to be an independent prognostic factor of colorectal cancer [54,55]. Although CRP is considered non-specific systemic marker of inflammation, many researchers have hypothesized that CRP may act as a biomarker for chronic low-grade intestinal inflammation and the subsequent development of colorectal cancer [56]. In this animal model, the development of intestinal tumors occurs early in life, therefore, there is a presence of constant chronic inflammation. Although the levels of CRP in the fecal samples were not significantly different at the last week of the experiment, there was an observed trend between control and treatment group, with higher levels determined in control group.

Growing evidence suggests that apoptosis is relevant in some infectious diseases by regulating immune responses [57]. As expected, we observed a high occurrence of cell turnover in the tumors found in aniamls treated with oxaliplatin. We detected only scarce amount of apoptotic cells on the surface of the tumor from control group animal, proving that the process of apoptosis is suppressed in inflamed tissue which allows cells with precancerous genetic mutations to live and grow into a cancer instead of having a normal, programmed cell death. Reduced mucin production in the intestine accompanies both inflammatory bowel disease and colon cancer and has been postulated as allowing irritation of the underlying epithelial cells by the intestinal microbiota [47]. We investigated the mucin production, a consequence of inflammatory state of the intestinal tissue by staining with alcian blue to detect mucous-producing Goblet cells. As predicted, an increased cell staining was observed in healthy, well-defined microvilli of the intestine, much decreased cells count within and around tumor areas. There is a strong evidence that NO itself, through its proinflammatory effects, may play an important role in carcinogenesis [48]. The increased production of nitric oxide could be a consequence of an increased level of oxidative stress, a consequence of the proinflammatory environment in the intestines of the mice.

We assessed the inflammatory changes in the small and large intestines' animals from control and treatment group by immunohistochemistry using cyclooxygenase-2 (Cox-2), cleaved caspase-3, Ki-67 and mdm-2 antibodies. Expression of Cox-2 is believed to play an important role in adenoma formation in murine polyposis models and is critical for the development of colorectal neoplasia [58]. Cox-2 expressing cells were mostly found in the tumors of control group animals, distributed throughout the entire tumors. COX-2 expression has a large impact on adenoma growth in *Apc*Min mice, where treatment with a COX-2-specific inhibitor is known to markedly reduce both the numbers and growth of adenomas. Furthermore, marked upregulation of COX-2 occurs in various cells including endothelial cells during stress and in inflammatory conditions such as sepsis. Caspase-3 is an enzyme crucial to the apoptotic process. Detection of activated caspase-3 is a valuable tool to identify dying cells even before morphological features of apoptosis are present [59]. Cleaved caspase-3 expressing cells were primarily expressed in apoptotic cells, apoptotic bodies and in some tumor cells of treatment group animals, mostly at the base and surface. They were localized to the nucleus and to the cytoplasm diffusely, thus they were fewer in the normal mucosa. In comparison with TUNEL method, cleaved caspase-3 staining was able to identify more apoptotic cells, most likely even pre-apoptotic cells. The Ki-67 nuclear

NIH-PA Author Manuscript

NIH-PA Author Manuscript

NIH-PA Author Manuscript

antigen is present throughout most of the cell cycle, and Ki-67 immunohistochemistry provides a reliable means of rapidly evaluating the growth fraction of normal and neoplastic cell populations [60]. Ki-67, a marker of proliferating cells, was highly expressed in adenomas of the control and treatment group, in both small and large intestine. We did not observed significant correlation in detection of apoptotic cells stained with cleaved caspase-3 and Ki-67. Mdm-2 gene amplification and overexpression occur in several types of tumors and are often associated with poor prognosis. Furthermore inhibition of mdm-2 expression enhances the activation of p53 by a DNA-damaging cancer chemotherapy agent in a synergistic fashion [49]. From immnuhistochemistry staining we detected increased levels of mdm-2 expressing cells in the control animal intestinal tissue as opposed to the treated condition.

5. Conclusions

In the present study, we designed a novel “particle in a particle” formulation where oxaliplatin was first loaded into nanoparticles composed of lipid like polymeric molecules which were later encapsulated in micro-sized alginate based particles. We believe that this combinatorial approach allowed for an improved and targeted delivery of the drug to the lower gastrointestinal tract where the tumor cells reside. This was confirmed after orally delivering formulation to the animals for 17 weeks which yielded in significant improvement in both tumor progression and morbidity when compared to control group. In summary, these findings confirm the previously reported potential of oxaliplatin in suppression and delaying of intestinal tumorigenesis. To our knowledge these are the first data to indicate that oral delivery of oxaliplatin induces reduction of protein concentration of proinflammatory cytokines, tumor burden, and morbidity when delivered orally. We believe this approach may have utility for the delivery of therapeutics to a variety of diseases in lower GI tract.

Acknowledgments

The authors would like to thank Abigail Scherer-Hoock, veterinary technician, for help with animals and helpful comments on this manuscript. We acknowledge post-doctoral fellowship from the Natural Sciences and Engineering Research Council (NSERC) to A. Urbanska. This work was supported by a grant from the National Institutes of Health Grant and Alnylam Pharmaceuticals.

References

1. Jemal A, Siegel R, Ward E, Murray T, Xu J, Smigal C, et al. Cancer statistics, 2006. CA Cancer J Clin. 2006; 56(2):106–130. [PubMed: 16514137]
2. Wang D, Lippard SJ. Cellular processing of platinum anticancer drugs. Nat Rev Drug Discov. 2005; 4(4):307–320. [PubMed: 15789122]
3. Wang X, Guo Z. Towards the rational design of platinum(II) and gold(III) complexes as antitumour agents. Dalton Trans. 2008; 28(12):1521–1532. [PubMed: 18335133]
4. Argyriou AA, Polychronopoulos P, Iconomou G, Chroni E, Kalofonos HP. A review on oxaliplatin-induced peripheral nerve damage. Cancer Treat Rev. 2008; 34(4):368–377. [PubMed: 18281158]
5. Rabik CA, Dolan ME. Molecular mechanisms of resistance and toxicity associated with platinating agents. Cancer Treat Rev. 2007; 33(1):9–23. [PubMed: 17084534]
6. Pietrangeli A, Leandri M, Terzoli E, Jandolo B, Garufi C. Persistence of highdose oxaliplatin-induced neuropathy at long-term follow-up. Eur Neurol. 2006; 56(1):13–16. [PubMed: 16825773]
7. Michor F, Iwasa Y, Lengauer C, Nowak MA. Dynamics of colorectal cancer. Semin Cancer Biol. 2005; 15(6):484–493. [PubMed: 16055342]
8. Nagda CD, Chotai NP, Nagda DC, Patel SB, Patel UL. Preparation and characterization of spray-dried mucoadhesive microspheres of ketorolac for nasal administration. Curr Drug Deliv. 2011; 21

NIH-PA Author Manuscript

NIH-PA Author Manuscript

NIH-PA Author Manuscript

9. Choi JS, Yoo HS. Pluronic/chitosan hydrogels containing epidermal growth factor with wound-adhesive and photo-crosslinkable properties. J Biomed Mater Res A. 2010; 95(2):564–573. [PubMed: 20725966]
10. Jain AK, Chalasani KB, Khar RK, Ahmed FJ, Diwan PV. Muco-adhesive multivesicular liposomes as an effective carrier for transmucosal insulin delivery. J Drug Target. 2007; 15(6):417–427. [PubMed: 17613660]
11. Wu SY, Chang HI, Burgess M, McMillan NA. Vaginal delivery of siRNA using a novel PEGylated lipoplex-entrapped alginate scaffold system. J Control Release. 2011; 155(3):418–426. [PubMed: 21315117]
12. Sahasathian T, Praphairaksit N, Muangsin N. Mucoadhesive and floating chitosan-coated alginate beads for the controlled gastric release of amoxicillin. Arch Pharm Res. 2010; 33(6):889–899. [PubMed: 20607494]
13. Cho WJ, Oh SH, Lee JH. Alginate film as a novel post-surgical tissue adhesion barrier. J Biomater Sci Polym Ed. 2010; 21(6):701–713. [PubMed: 20482979]
14. Penman A, Sanderson GR. A method for the determination of uronic acid sequence in alginates. Carbohydr Res. 1972; 25(2):273–282. [PubMed: 4679629]
15. (FDA) UFaDA. Food additive status list. 2006
16. Igoe, RS. Dictionary of food ingredients. 4th ed.. New York: Van Nostrand Reinhold Co, cop; 1983.
17. Wheatley MA, Chang M, Park E, Langer R. Coated alginate microspheres - factors influencing the controlled delivery of macromolecules. J Appl Polym Sci. 2003; 43(11):2123–2135.
18. Kim CK, Lee EJ. The controlled release of blue dextran from alginate beads. Int J Pharm. 1992; 79(1):11–19.
19. Singh ON, Burgess J. Characterization of albumin-alginic acid complex coacervation. J Pharm Pharmacol. 1989; 41(10):670–673. [PubMed: 2575142]
20. Baldwin AD, Kiick KL. Polysaccharide-modified synthetic polymeric biomaterials. Biopolymers. 2010; 94(1):128–140. [PubMed: 20091875]
21. Tonnesen HH, Karlsen J. Alginate in drug delivery systems. Drug Dev Ind Pharm. 2002; 28(6): 621–630. [PubMed: 12149954]
22. Peters MC, Isenberg BC, Rowley JA, Mooney DJ. Release from alginate enhances the biological activity of vascular endothelial growth factor. J Biomater Sci Polym Ed. 1998; 9(12):1267–1278. [PubMed: 9860169]
23. Sharma CP, Paul W. Chitosan, a drug carrier for the 21st century: a review. Stp Pharma Sci. 2000; 10(1):5–22.
24. Su LK, Kinzler KW, Vogelstein B, Preisinger AC, Moser AR, Luongo C, et al. Multiple intestinal neoplasia caused by a mutation in the murine homolog of the APC gene. Science. 1992; 256(5057):668–670. [PubMed: 1350108]
25. Love KT, Mahon KP, Levins CG, Whitehead KA, Querbes W, Dorkin JR, et al. Lipid-like materials for low-dose, in vivo gene silencing. Proc Natl Acad Sci USA. 2010; 107(5):1864–1869. [PubMed: 20080679]
26. Huerta S, Irwin RW, Heber D, Go VL, Moatamed F, Ou C, et al. Intestinal polyp formation in the Apcmin mouse: effects of levels of dietary calcium and altered vitamin D homeostasis. Dig Dis Sci. 2003; 48(5):870–876. [PubMed: 12772782]
27. Terhaar Sive Droste JS, Craanen ME, van der Hulst RW, Bartelsman JF, Bezemer DP, Cappendijk KR, et al. Colonoscopic yield of colorectal neoplasia in daily clinical practice. World J Gastroenterol. 2009; 15(9):1085–1092. [PubMed: 19266601]
28. Rominiyi O, Broman DM, Rajaganeshan R, Selvasekar CR. Colon cancer presenting with polymyositis-A case report. Int J Surg Case Rep. 2011; 2(7):225–227. [PubMed: 22096734]
29. Sharma S, Longo WE, Baniadam B, Vernava 3rd AM. Colorectal manifestations of endocrine disease. Dis Colon Rectum. 1995; 38(3):318–323. [PubMed: 7882801]
30. Mecklenburg I, Leibig M, Weber C, Schmidbauer S, Folwaczny C. Recurrent severe gastrointestinal bleeding and malabsorption due to extensive habitual megacolon. World J Gastroenterol. 2005; 11(48):7686–7687. [PubMed: 16437700]

NIH-PA Author Manuscript

NIH-PA Author Manuscript

NIH-PA Author Manuscript

31. MacDermott RP. Alterations of the mucosal immune system in inflammatory bowel disease. J Gastroenterol. 1996; 31(6):907–916. [PubMed: 9027661]
32. McClellan JL, Davis JM, Steiner JL, Day SD, Steck SE, Carmichael MD, et al. Intestinal inflammatory cytokine response in relation to tumorigenesis in the Apc(Min/+) mouse. Cytokine. 2011; 57(11):113–119. [PubMed: 22056354]
33. Playford RJ, Ghosh S. Cytokines and growth factor modulators in intestinal inflammation and repair. J Pathol. 2005; 205(4):417–425. [PubMed: 15714466]
34. Fuss IJ. Cytokine network in inflammatory bowel disease. Curr Drug Targets Inflamm Allergy. 2003; 2(2):101–112. [PubMed: 14561161]
35. Judd TA, Day AS, Lemberg DA, Turner D, Leach ST. Update of fecal markers of inflammation in inflammatory bowel disease. J Gastroenterol Hepatol. 2011; 26(10):1493–1499. [PubMed: 21777275]
36. Lee S, Choe JW, Kim HK, Sung J. High-sensitivity C-reactive protein and cancer. J Epidemiol. 2011; 21(3):161–168. [PubMed: 21368452]
37. Kim DK, Oh SY, Kwon HC, Lee S, Kwon KA, Kim BG, et al. Clinical significances of preoperative serum interleukin-6 and C-reactive protein level in operable gastric cancer. BMC Cancer. 2009; 9:155. [PubMed: 19457231]
38. Scagliotti GV, De Marinis F, Rinaldi M, Crino L, Gridelli C, Ricci S, et al. Phase III randomized trial comparing three platinum-based doublets in advanced nonsmall- cell lung cancer. J Clin Oncol. 2002; 20(21):4285–4291. [PubMed: 12409326]
39. Monk BJ, Sill MW, McMeekin DS, Cohn DE, Ramondetta LM, Boardman CH, et al. Phase III trial of four cisplatin-containing doublet combinations in stage, IVB, recurrent, or persistent cervical carcinoma: a Gynecologic Oncology Group study. J Clin Oncol. 2009; 27(28):4649–4655. [PubMed: 19720909]
40. Zachos I, Konstantinopoulos PA, Tzortzis V, Gravas S, Karatzas A, Karamouzis MV, et al. Systemic therapy of metastatic bladder cancer in the molecular era: current status and future promise. Expert Opin Investig Drugs. 2010; 19(7):875–887.
41. Moser AR, Pitot HC, Dove WF. A dominant mutation that predisposes to multiple intestinal neoplasia in the mouse. Science. 1990; 247(4940):322–324. [PubMed: 2296722]
42. Perkins S, Verschoyle RD, Hill K, Parveen I, Threadgill MD, Sharma RA, et al. Chemopreventive efficacy and pharmacokinetics of curcumin in the min/+ mouse, a model of familial adenomatous polyposis. Cancer Epidemiol Biomarkers Prev. 2002; 11(6):535–540. [PubMed: 12050094]
43. Corpet DE, Pierre F. Point: from animal models to prevention of colon cancer.Systematic review of chemoprevention in min mice and choice of the model system. Cancer Epidemiol Biomarkers Prev. 2003; 12(5):391–400. [PubMed: 12750232]
44. Sethi G, Shanmugam MK, Ramachandran L, Kumar AP, Tergaonkar V. Multifaceted link between cancer and inflammation. Biosci Rep. 2012; 32(1):1–15. [PubMed: 21981137]
45. Lowe DB, Storkus WJ. Chronic inflammation and immunologic-based constraints in malignant disease. Immunotherapy. 2011; 3(10):1265–1274. [PubMed: 21995576]
46. Hakansson A, Branning C, Molin G, Adawi D, Hagslatt ML, Nyman M, et al. Colorectal oncogenesis and inflammation in a rat model based on chronic inflammation due to cycling DSS treatments. Gastroenterol Res Pract. 2011:924045. [PubMed: 22007198]
47. Macarthur M, Hold GL, El-Omar EM. Inflammation and cancer II. Role of chronic inflammation and cytokine gene polymorphisms in the pathogenesis of gastrointestinal malignancy. Am J Physiol Gastrointest Liver Physiol. 2004; 286(4):G515–G520. [PubMed: 15010360]
48. Langholz E, Munkholm P, Davidsen M, Binder V. Course of ulcerative colitis: analysis of changes in disease activity over years. Gastroenterology. 1994; 107(1):3–11. [PubMed: 8020674]
49. Kinoshita T, Ito H, Miki C. Serum interleukin-6 level reflects the tumor proliferative activity in patients with colorectal carcinoma. Cancer. 1999; 85(12):2526–2531. [PubMed: 10375098]
50. Tomita M, Wakabayashi H, Yamauchi K, Teraguchi S, Hayasawa H. Bovine lactoferrin and lactoferricin derived from milk: production and applications. Biochem Cell Biol. 2002; 80(1):109–112. [PubMed: 11908633]

NIH-PA Author Manuscript

NIH-PA Author Manuscript

NIH-PA Author Manuscript

51. Sugi K, Saitoh O, Hirata I, Katsu K. Fecal lactoferrin as a marker for disease activity in inflammatory bowel disease: comparison with other neutrophilderived proteins. Am J Gastroenterol. 1996; 91(5):927–934. [PubMed: 8633583]
52. Kane SV, Sandborn WJ, Rufo PA, Zholudev A, Boone J, Lyerly D, et al. Fecal lactoferrin is a sensitive and specific marker in identifying intestinal inflammation. Am J Gastroenterol. 2003; 98(6):1309–1314. [PubMed: 12818275]
53. Baveye S, Elass E, Mazurier J, Spik G, Legrand D. Lactoferrin: a multifunctional glycoprotein involved in the modulation of the inflammatory process. Clin Chem Lab Med. 1999; 37(3):281–286. [PubMed: 10353473]
54. Shiu YC, Lin JK, Huang CJ, Jiang JK, Wang LW, Huang HC, et al. Is C-reactive protein a prognostic factor of colorectal cancer? Dis Colon Rectum. 2008; 51(4):443–449. [PubMed: 18172726]
55. van de Poll MC, Klaver YL, Lemmens VE, Leenders BJ, Nienhuijs SW, de Hingh IH. C-reactive protein concentration is associated with prognosis in patients suffering from peritoneal carcinomatosis of colorectal origin. Int J Colorectal Dis. 2011; 26(8):1067–1073. [PubMed: 21476028]
56. Dymicka-Piekarska V, Matowicka-Karna J, Gryko M, Kemona-Chetnik I, Kemona H. Relationship between soluble P-selectin and inflammatory factors (interleukin-6 and C-reactive protein) in colorectal cancer. Thromb Res. 2007; 120(4):585–590. [PubMed: 17169411]
57. Dockrell DH. Apoptotic cell death in the pathogenesis of infectious diseases. J Infect. 2001; 42(4): 227–234. [PubMed: 11545564]
58. Oshima M, Taketo MM. COX selectivity and animal models for colon cancer. Curr Pharm Des. 2002; 8(12):1021–1034. [PubMed: 11945149]
59. Arai M, Sasaki A, Saito N, Nakazato Y. Immunohistochemical analysis of cleaved caspase-3 detects high level of apoptosis frequently in diffuse large Bcell lymphomas of the central nervous system. Pathol Int. 2005; 55(3):122–129. [PubMed: 15743320]
60. Gerdes J, Dallenbach F, Lennert K, Lemke H, Stein H. Growth fractions in malignant non-Hodgkin's lymphomas (NHL) as determined in situ with the monoclonal antibody Ki-67. Hematol Oncol. 1984; 2(4):365–371. [PubMed: 6396192]

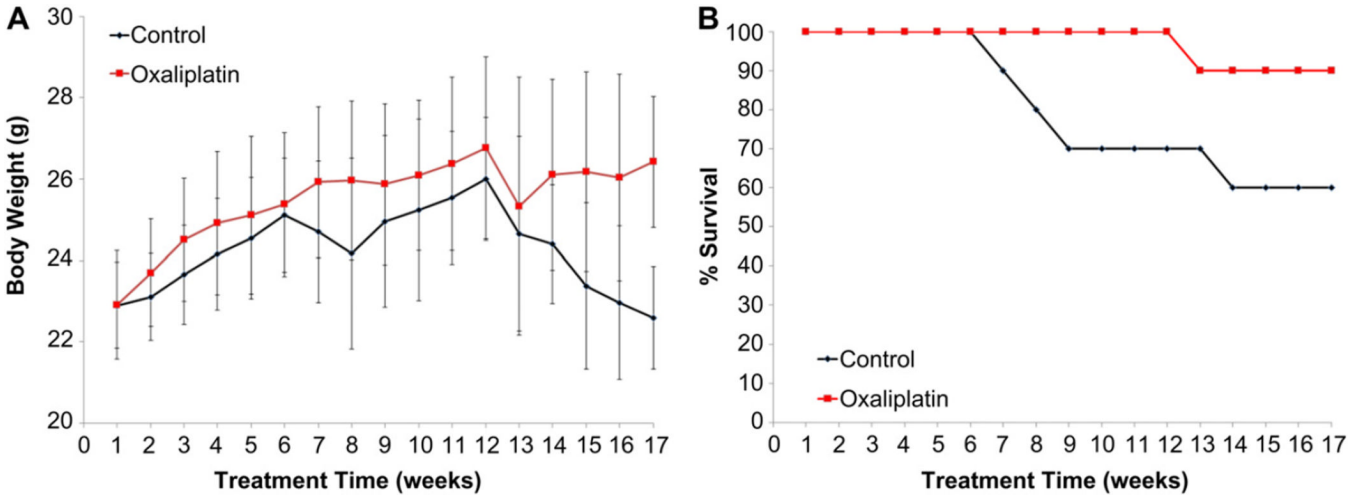

Fig. 1.

Animal body weights over 17-week trial; control group – animals gavaged with empty alginate-chitosan (AC) microcapsules suspended in PBS, treatment group – animals gavaged with AC microencapsulated lipidoid and oxaliplatin nanoparticles suspended in PBS (A); Animal survival profile (B).

NIH-PA Author Manuscript NIH-PA Author Manuscript NIH-PA Author Manuscript

NIH-PA Author Manuscript
NIH-PA Author Manuscript
NIH-PA Author Manuscript

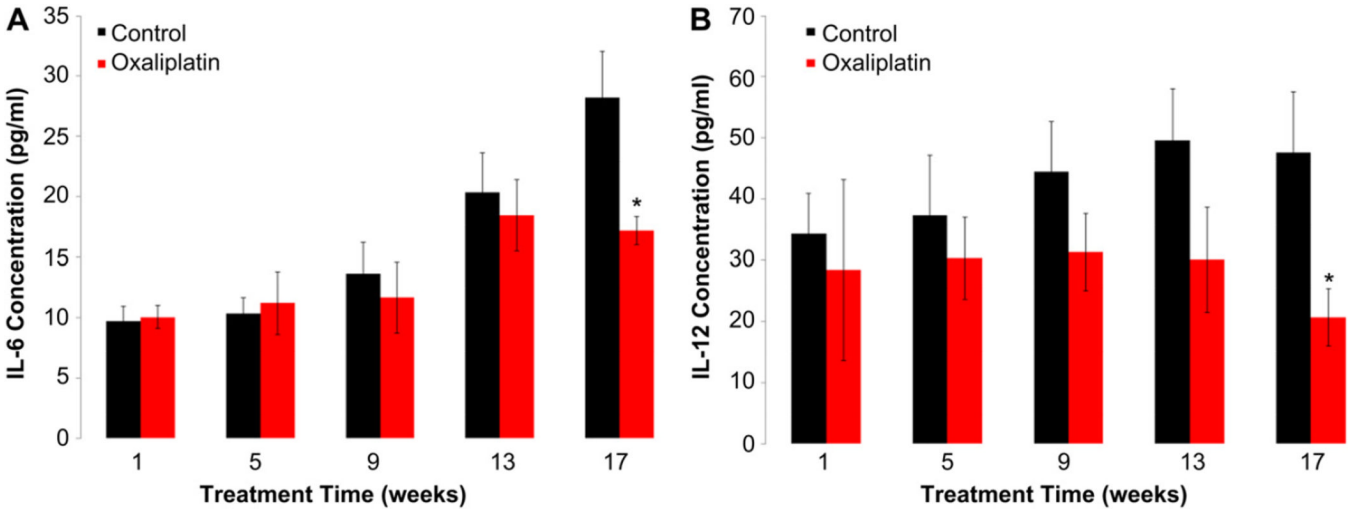

Fig. 2.

The effect of treatments on IL-12 concentrations in serum (A) and IL-6 concentrations in serum (B) in animals, Control group – animals gavaged with empty alginatechitosan (AC) microcapsules suspended in PBS, Treatment group – animals gavaged with AC microencapsulated lipidoid and oxaliplatin nanoparticles suspended in PBS. Data represent the mean ± SD of concentration levels per group. Asterisks: statistical differences ($p < .05$) when compared to control.

NIH-PA Author Manuscript
NIH-PA Author Manuscript
NIH-PA Author Manuscript

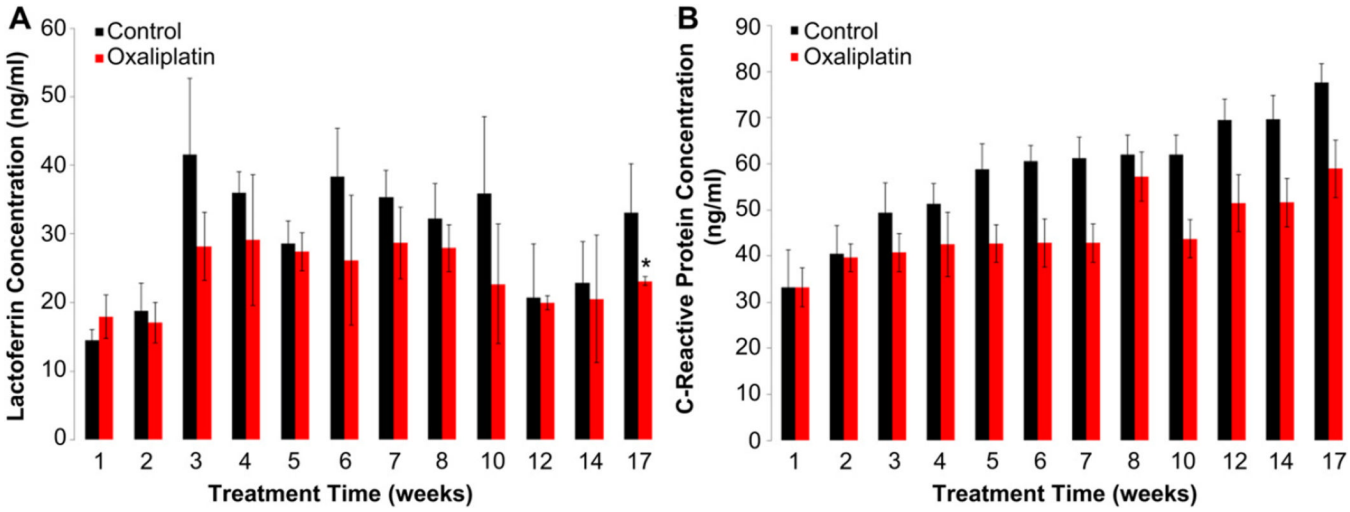

Fig. 3.

The effect of treatments on lactoferrin concentrations (3A) and C-reactive protein (3B) in fecal samples of animals, Control group – animals gavaged with empty alginatechitosan (AC) microcapsules suspended in PBS, Treatment group – animals gavaged with AC microencapsulated lipidoid and oxaliplatin nanoparticles suspended in PBS. Data represent the mean ± SD of concentration levels per group. Asterisks: statistical differences ($p < .05$) when compared to control.

NIH-PA Author Manuscript
NIH-PA Author Manuscript
NIH-PA Author Manuscript

Fig. 4.

H&E tissue staining of mice polyps in small intestine, colon and cecum for control and oxaliplatin treatment group. Control mice had a higher number of polyps, indicated with red arrows, in the small intestine, colon and cecum compared with oxaliplatin treatment group. (For interpretation of the references to colour in this figure legend, the reader is referred to the web version of this article.)

NIH-PA Author Manuscript
NIH-PA Author Manuscript
NIH-PA Author Manuscript

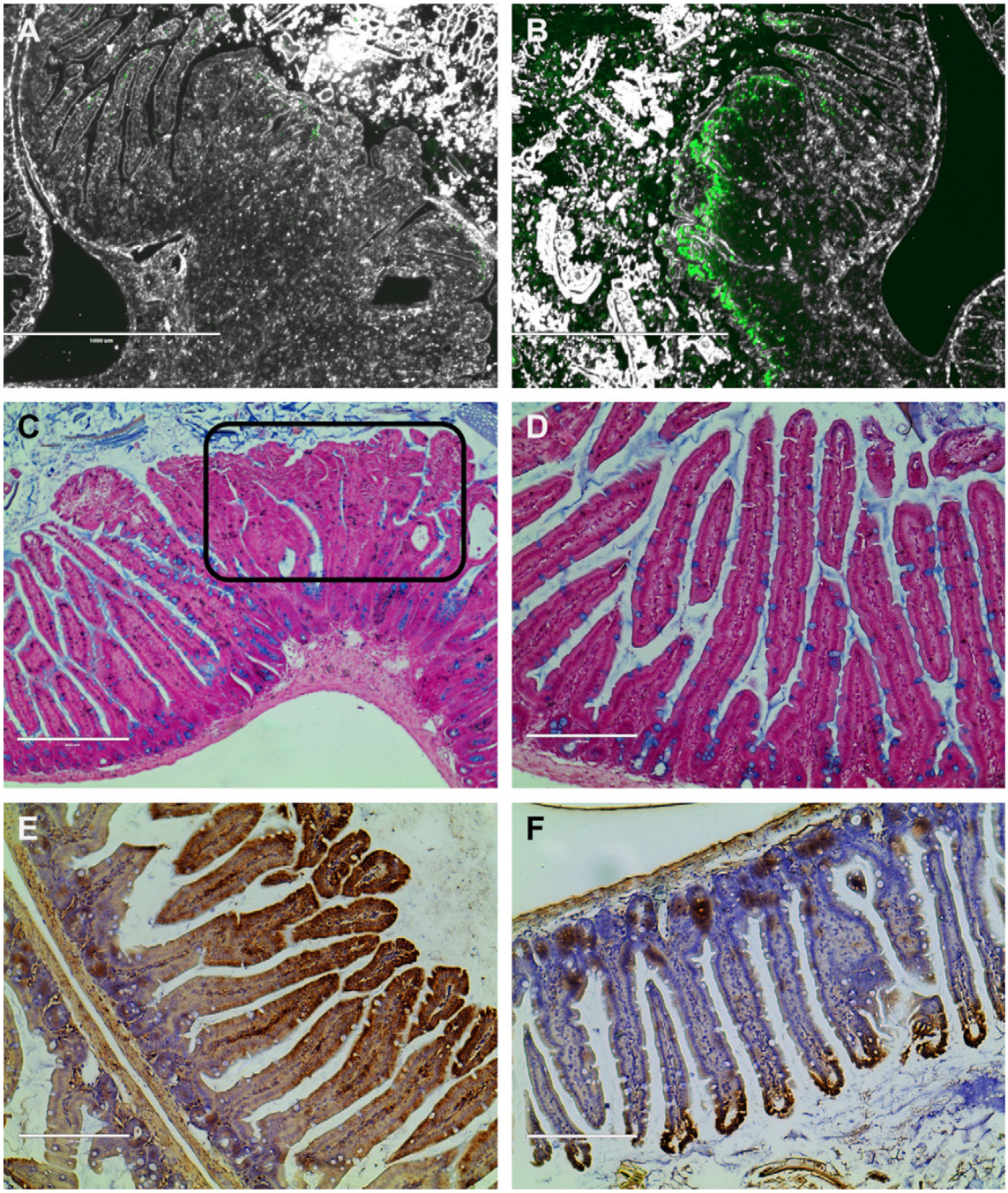

Fig. 5.

Terminal deoxynucleotidyl transferase-Mediated dUTP nick end labeling, representative tumor from control group animal (A) and oxaliplatin treatment (B); alcian blue staining of Goblet cells shows reduced mucin production within adenoma (C) compared to normal intestinal tissue expressing mucin producing cells (D); evidence of increased nitrosative stress in control group animals showing intestinal microvilli (E) relative to microvilli obtained from treatment group animal (F); magnification 4×.

NIH-PA Author Manuscript
NIH-PA Author Manuscript
NIH-PA Author Manuscript

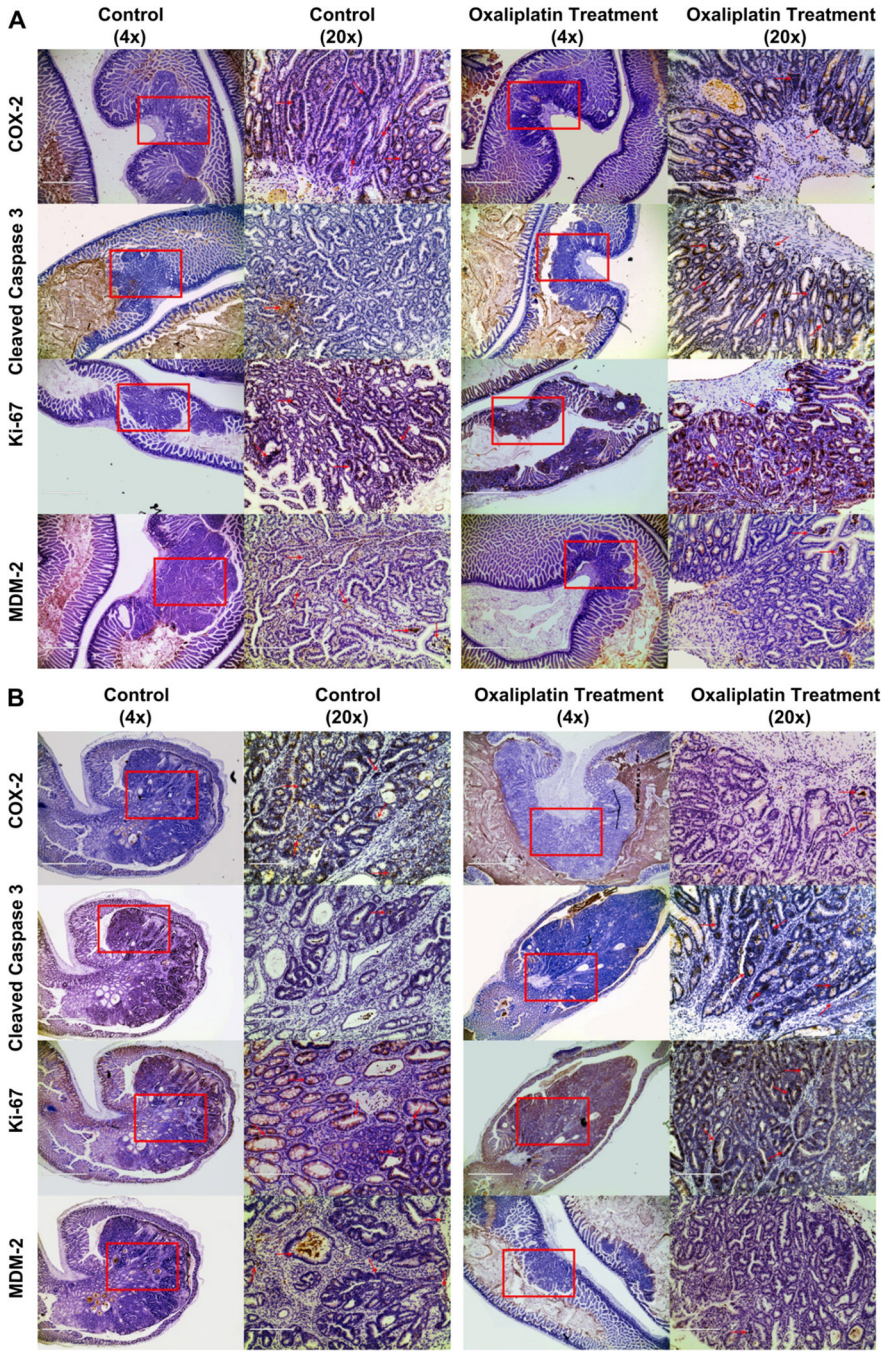

Fig. 6.

Immunohistochemical analysis of adenomas found in the small intestine (A) and colon (B) stained for Cox-2, Cleaved Caspase-3, Ki-67 and Mdm-2. Each panel compares adenomas found in the control and treatment group. Section magnified is selected in a red rectangle and stained cells are pointed out with red arrows. All shown sections are at 4× magnification (bar = 1000um) and further magnified to show details at 20× (bar = 100 um). Immunohistochemistry was performed using Cox-2 (Santa Cruz, CA), Cleaved Caspase-3 (Cell Signaling), Ki-67 (Dako) and Mdm-2 (Santa Cruz, CA) antibodies at a 1:500 dilution. Immunohistochemical signal was detected by secondary biotinylated goat anti-mouse antibody (1:500 dilution; Santa Cruz, CA) followed by Vector ABC tertiary kit (Vector

NIH-PA Author Manuscript

NIH-PA Author Manuscript

NIH-PA Author Manuscript

Laboratories, Burlingame, CA, USA) according to the manufacturer's instructions. All immunohistochemistry was performed on a BondMax machine (Vision Biosystems, Newcastle, UK) according to the manufacturer's instructions and involved antigen retrieval by BondMax Epitope retrieval solution heated on the machine for 20 min. (For interpretation of the references to colour in this figure legend, the reader is referred to the web version of this article.)

NIH-PA Author Manuscript NIH-PA Author Manuscript NIH-PA Author Manuscript

Table 1

Enumeration, classification (A) and scoring (B) of tumors in animals. Spleen weights and lengths among groups (C).

(A)

	Control (6)			Treatment (9)		
	Small intestine	**Cecum**	**Colon**	**Small intestine**	**Cecum**	**Colon**
GIN	65	2	0	69	1	4
Adenoma	26	0	6	22	0	1
Total	91	2	6	91	1	4
Avg/animal	15.2	0.33	1	10.11	0.11	0.44

(B)

Group (*n*)	**Tumor scores in group and per animal**		
	Small intestine	**Colon**	**Total**
Control (6)	4	2	4
	4	2	4
	3	2	4
	3	2	4
	3	0	4
	4	2	4
Avg/animal	3.5 ± 0.20	1.6 ± 0.44	4±0.00
Treatment (9)	2	0	2
	1	0	1
	2	1	3
	2	0	2
	4	1	4
	2	2	2
	3	3	3
	2	2	4
	2	2	4
Avg/animal	2.2 ± 0.25	1.2 ± 0.20	2.8±0.26

Biomaterials. Author manuscript; available in PMC 2013 March 03.

NIH-PA Author Manuscript

NIH-PA Author Manuscript

NIH-PA Author Manuscript

(C)

	Spleen	
	Length (cm)	**Weight (mg)**
Control (6)	2.33 ± 0.25	485 ± 8.21
Treatment (9)	2.28 ± 0.14	404 ± 10.08